Fizika Nizkikh Temperatur, 2003, v. 29, Nos. 9/10, p. 992–1000

Tunneling dynamics in cryocrystals: localization and delocalization

Vyacheslav G. Storchak

Russian Research Centre «Kurchatov Institute», 46 Kurchatov Sq., Moscow 123182, Russia
E-mail: storchak@dnus.polyn.kiae.su

The phenomenon of quantum diffusion of muonium in cryocrystals with rotational degrees of freedom is discussed. The quantum tunneling dynamics and electron transport are considered taking into account the effects of disorder.

PACS: 67.40.Yv, 73.20.Jc

1. Introduction

A vast amount of kinetic processes in chemistry and biology, nuclear and solid state physics, disordered systems and liquids, etc. deals with the mass and charge transport, i.e. dynamics of neutral (typically atomic) particles and charged particles (typically electrons or electronic complexes), limited by potential barriers. At low temperatures there is no other way to overcome a potential barrier than by quantum tunneling of a particle through it. This phenomenon is called quantum diffusion (QD). The concept of quantum diffusion is introduced for diffusing particles which are heavy compared with electron. On the other hand, a quantum-mechanical evaluation suggests that the tunneling probability is crucially enhanced for light particles. Therefore, in the context of QD the role of the positive muon (μ^+) is of particular interest because of its intermediate mass (about 200 times more than that of the electron, but about an order of magnitude less than that of the proton). Being a complete chemical analogue of the proton, μ^+ captures an electron and forms the light hydrogen isotope known as muonium ($Mu = \mu^+ + e^-$). This happens in insulators and semiconductors, while in metals we deal with the «bare» muon. Because of the unique mass of the muon one can hardly mention any other example where quantum diffusion was observed in such a wide temperature range as for μ^+ and Mu [1]. The other reason for the success of the quantum diffusion study using muons is the sensitivity of the muon spin relaxation (μSR) techniques (see e.g. [2]) to μ^+ and Mu dynamics.

The basic issue in nonclassical transport is whether a wave-like or particle-like description is appropriate, i.e., whether the tunneling is coherent or incoherent. This depends on whether the interaction with the environment is such as to lead to spatial localization of the wave function or to bandlike (Bloch wave) motion. One of the possible channels for localization of a particle is through its interaction with lattice excitations (phonons, librons, magnons etc.). In a dissipative environment [3] the lattice excitations can be represented as a bath of harmonic oscillators; interaction with this environment causes a crossover from coherent quantum tunneling to incoherent hopping dynamics when the particle «dressed» with the lattice excitations can be effectively thought of as a polaron.

At low temperatures, the environmental excitations are frozen out. In this case, conventional understanding suggests that the only possible channel for particle localization is the introduction of crystal disorder, which thus may dramatically change the transport properties of a solid. A well-known example is the spatial localization of electron states near the Fermi level in a disordered metallic system, which leads to a transition into a dielectric state (the Anderson transition) [4]. The concept of Anderson localization suggests that the wave function of a particle in a random potential may change qualitatively if the randomness becomes large enough. Coherent tunneling of a particle is possible only between levels with the same energy (e.g. between equivalent sites); in the case of strong randomness, states with the same energy may be too distant (spatially separated) for tunneling to be effective.

Although the concept of localization by disorder has been introduced primarily in order to describe the electronic transport properties of condensed matter, it may also be applied to the quantum dynamics of heavier particles, whether charged or neutral [5,1]. Recent experimental results for positive muons as well

as for muonium atoms clearly indicated that interaction with crystal excitations and crystal disorder dramatically changes the nature of tunneling dynamics for particles ~ 200 times heavier than the electron.

In this lecture we discuss recent studies on both quantum tunneling dynamics and electron transport in cryocrystals using μ^+SR techniques paying particular attention to processes of particle localization and delocalization.

2. Quantum diffusion via μ^+SR

Under-the-barrier tunneling dynamics of particles in crystalline lattice is pure quantum mechanical phenomenon which has no analogue in classical physics. Typically, tunneling occurs between two or more potential wells which would be degenerate in a pure system. In this case the quantum-mechanical coherence between the particle's states in different wells manifests itself (the well-known example is the Bloch wave propagation of electrons in crystalline solids). The basic concept introduced to describe this phenomenon is that of a band motion (coherent tunneling) of a particle with a bandwidth Δ determined by the amplitude of the particle's resonance transitions between the potential minima [6,7]. Particle dynamics in perfect crystal at $T = 0$ presents the simplest case of a band motion. The standard expression for the tunneling amplitude between the two nearest wells is given in the semiclassical approximation (see, e.g., [8], $\hbar = 1$)

$$\Delta = 2Z\nu_0 e^{-S_0} . \qquad (1)$$

Here we assume that for the particle with the mass $m >> m_e$, where m_e is the electron mass, zero-point vibrations ZPV around local minima of the crystal potential are small as compared with the interwell separation a (or lattice constant, if there is only one minimum in the unit cell). This condition implies that tunneling splitting of the lowest levels in each well is much less then ZVP frequency $\omega_0 = 2\pi\nu_0$, and the lowest states are well separated from the rest of the particle spectrum. The tunneling action $S_0 = \int_{\mathbf{r}_1}^{\mathbf{r}_2} p\mathrm{d}x$ is given by the integral along the optimal path connecting turning points $\mathbf{r}_1$ and $\mathbf{r}_2$ on different sides of the barrier; Z being the coordination number.

Typically, in solids $S_0 >> 1$ which in fact is already satisfied when the barrier height U_B is only few times larger than the ZPV energy [1]. Therefore even for particles with the intermediate mass like muons or muonium atoms the bandwidth turns out to be exponentially small. Nevertheless, at $T = 0$ in a perfect crystal any particle is completely delocalized.

At $T \neq 0$, however, tunneling occurs on the background of the coupling with the excitations of the medium. Since Δ is so small the interaction of the particle with environmental excitations may easily destroy the coherence and lead to particle localization. The basic characteristic of the particle interactions with the medium excitations is frequency Ω of phase correlations damping at neighboring equivalent positions of the particle. Even at low temperatures Ω could be as large as Δ; the temperature raise results in an exponential decrease of the coherent tunneling transition [5,1].

Here one have to distinguish different frequency regimes: those modes which have frequencies significantly larger than Δ will follow the motion of the particle adiabatically and can at best renormalize Δ; while those of frequencies of order of Δ or less can extract energy from the system during the tunneling process. The latter effect is known as dissipation in quantum tunneling [3,9] which causes strong particle localization. Destraction of bandlike propagation and eventual localization of muonium atom in molecular crystals of solid methanes [10] and solid nitrogen [11] due to coupling to molecular rotations at low temperatures are typical examples of this kind of effect: interaction with low-frequency rotational modes causes the crossover from coherent quantum tunneling to incoherent hopping dynamics at low temperatures.

Since Δ is small with respect to all other energy parameters in a solid, quantum dynamics is extremely sensitive to crystal imperfections. Therefore, localization of the particle often takes place at a relatively low defect concentration.

Until very recently studies of Mu diffusion have focussed on nearly perfect crystals, in which bandlike motion of Mu persists at low temperatures. Crystalline defects have been treated mainly as local traps [12] with trapping radii on the order of the lattice constant a. The justification for such an approach was that the characteristic energy of the crystalline distortion, $U(a)$, is usually much less than the characteristic energy of lattice vibrations, Θ. Unfortunately, since it does not take the particle bandwidth Δ into consideration, this comparison turns out to be irrelevant to the problem of particle dynamics, for which the crucial consideration is that Δ is usually several orders of magnitude less than $U(a)$. For example, a typical Mu bandwidth in insulators is on the order of $\Delta \sim 0.01$–0.1 K [1], whereas $U(a)$ could be as large as 10 K. In metals the mismatch is even more drastic: typical values [$U(a) \sim 10^3$ K vs. $\Delta \sim 10^{-4}$ K] differ by about seven orders of magnitude. Under these circumstances, the influence of crystalline defects extends over distances much larger than a. If the «disturbed» regions around defects overlap sufficiently, complete particle localization can result.

In this lecture we concentrate our attention on Mu quantum diffusion phenomena in cryocrystals with rotational degrees of freedom. A more general review of muon and muonium diffusion in a variety of materials may be found elsewhere [1].

2.1. Destruction of bandlike propagation in orientationally ordered crystals: the two-phonon quantum diffusion regime

Studies of the diffusion of hydrogen atoms [15] and μ^+ in metals, as well as Mu diffusion in insulators and semiconductors [1] have convincingly shown the quantum mechanical character of the phenomenon, most clearly seen at low temperatures where the particle hop rate τ_c^{-1} increases with decreasing temperature T according to the power law $\tau_c^{-1} \propto T^{-\alpha}$, thus manifesting the onset of the coherent process. In metals, coupling to conduction electrons is the dominant scattering mechanism [16] and causes $\alpha < 1$. In insulators, where phonon scattering processes prevail, a is predicted [5,6] to be 7 or 9 at low temperatures where the absorption of single phonons shifts the energy of the diffusing particle too much for tunneling to occur and so two-phonon diagrams (which can leave the energy almost unchanged) are expected to dominate. Surprisingly, the experimental results on Mu diffusion in ionic insulators [17] indicate that α is generally close to 3; this «universal» power-law behaviour with $\alpha \approx 3$ prompted the authors of Ref. l8 to conclude that muonium diffusion is governed by one-phonon scattering. On the other hand, in Ref. 19 it was shown that $\alpha \approx 3$ can also be obtained from two-phonon scattering processes if the actual phonon spectrum of the ionic crystal is taken into account; unfortunately that procedure requires introduction of adjustable parameters. This basic problem on the validity of the former or the latter remained open until recent results on Mu quantum diffusion in solid nitrogen [11], methanes [10], and carbon dioxide [20] presented direct experimental evidence of the dominance of two-phonon scattering mechanism in insulators at low temperatures.

In the harmonic approximation, the transport properties of a neutral particle in a simple crystalline insulator (e.g. a monatomic or ionic crystal) depend only on the phonon modes of the lattice. For crystals composed of molecules, two additional contributions enter from the internal vibrational and rotational degrees of freedom of the molecules. Internal vibrations of molecules scarcely change the particle dynamics because of their extremely high frequencies. Molecular rotation, however, is a different matter. Two extremes are possible: the molecules may rotate almost freely in the crystal or the rotational motion may be severely restricted and hence transformed into torsional excitations (librons). Since typical rotational frequencies are still much higher than the particle bandwidth, in the first extreme the energy levels in different unit cells are degenerate and therefore particle dynamics remain unperturbed. In the second extreme the anisotropic interaction between molecules (which causes orientational ordering in the first place) changes the crystalline potential so that this degeneracy is lifted. As far as the particle dynamics are concerned, this splitting of the energy levels of adjacent sites acts as an effective disorder, creating the bias ξ. To demonstrate this, a suitable molecular lattice should be found where (a) this disorder is essentially weak and short range and (b) both extremes can be reached in the accessible temperature range. The simplest molecular solids are the cryocrystals formed by the small lightweight molecules, namely solid H_2, D_2, CH_4, CD_4, N_2, N_2O, CO_2 etc. In solid N_2O and CO_2 the anisotropic part of intermolecular interaction is so strong that the lattice keeps its orientational order in the entire solid phase. In solid para-H_2 and ortho-D_2, by contrast, this interaction is so weak that orientational order cannot be reached even at the lowest temperatures. Here we discuss our study of muonium dynamics in solid nitrogen and methanes (CH_4 and CD_4) which undergo orientational ordering in the solid phase. In solid N_2 this transition takes place at $T = 35.6$ K, in CH_4 – at $T = 20.4$ K while in solid CD_4 partial orientational ordering occurs at $T = 27$ K with a further transition to complete molecular ordering at $T = 22.1$ K. These crystals show similar nonmonotonic temperature dependences of muonium relaxation rate T_2^{-1}. Figure 1 presents the temperature dependence of the muonium hop rate τ_c^{-1} in solid nitrogen. For temperatures $T << \Theta$ (the Debye temperature) quantum diffusion is believed [5] to be governed by two-phonon processes, for which τ_c^{-1} is given by

$$\tau_c^{-1} \sim \frac{\tilde{\Delta}_0^2 \Omega(T)}{\Omega^2(T) + \xi^2}, \qquad (2)$$

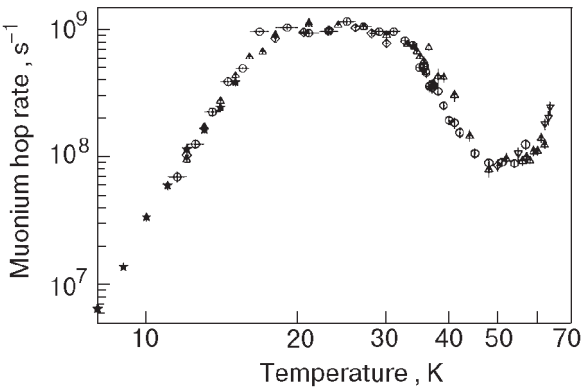

Fig.1. Temperature dependence of the muonium hop rate in ultra high purity solid N_2. Stars correspond to the combined longitudinal field measurements; circles, triangles, diamonds and inverted triangles correspond to transverse field measurements in different samples.

where $\tilde{\Delta}_0$ is the renormalized bandwidth for Mu diffusion and ξ is the typical difference between energy levels of the particle at adjacent tunneling sites due to static disorder.

The-main feature of Eq. (2) is the minimum of $\tau_c(T)$ at $\xi \sim \Omega(T)$.

Note that

$$\tau_c^{-1} \propto \frac{\tilde{\Delta}_0^2}{\Omega(T)} \quad \text{for} \quad \xi < \Omega, \tag{3}$$

$$\text{whereas} \quad \tau_c^{-1} \propto \frac{\tilde{\Delta}_0^2\,\Omega(T)}{\xi^2} \quad \text{for} \quad \xi >> \Omega \tag{4}$$

giving the opposite temperature dependence so that Mu atoms are localized as $T \to 0$. In the $T \to 0$ limit only acoustic phonons are important and

$$\Omega(T) \propto T^{7(+2)} \tag{5}$$

The two additional powers of T appear only in the case of muonium tunneling between absolutely equivalent sites.

In the temperature range 30 K < T < 50 K, the measured Mu hop rate in solid nitrogen exhibits an empirical temperature dependence $\tau_c^{-1} \propto T^{-\alpha}$ with α = 7.3(2); since, from Eq. (3), $\tau_c^{-1} \propto \Omega^{-1}(T)$, we have $\Omega(T) \propto T^7$ as expected [Eq. (5)]. This is the first experimental confirmation of the T^{-7} dependence of τ_c^{-1} predicted by the two-phonon theory of quantum diffusion [5].

Below about 30 K the Mu, hop rate levels off, due to band motion with an estimated [11] renormalized bandwidth of $\tilde{\Delta}_0 \sim 10^{-2}$ K [11]. Similar experiments in solid methanes give the following values for muonium bandwidth: about $3 \cdot 10^{-2}$ K in CH_4 and about 10^{-3} K in CD_4. This values for the Mu bandwidth in solid nitrogen and methanes should be compared with the bandwidth $\Delta \sim 10^{-4}$ K obtained for the quantum diffusion of ^{3}He atoms in ^{4}He crystals [21]: the qualitative similarity of these results suggests a common dynamical behaviour for light particles in insulators, as opposed to metals, where different scattering mechanisms lead to quite different impurity dynamics.

Muonium motion in solid nitrogen slows down again below about 20 K, probably due to the orientational ordering of N_2 molecules. For T < 18 K the data in Fig. l obey

$$\tau_c^{-1} = \tau_0^{-1}\left(\frac{T}{\Theta}\right)^{\alpha}, \tag{6}$$

with Θ = 83 K, $\tau_0^{-1} = 3.6(8) \cdot 10^{13}\ \text{s}^{-1}$ and α = 6.7(1).

The change in the temperature dependence of the Mu hop rate from a T^7 to a T^{-7} law reflects a crossover from Eq. (3) to Eq. (4). Muonium diffusion in solid methane isotopes and solid carbon dioxide exhibits similar temperature dependences of τ_c^{-1} [10,20]. In all four crystals, at low temperatures gradual Mu localization takes place which reflects a suppression of band motion by static disorder introduced by orientational ordering.

2.2. Coherent quantum diffusion of muonium atom in highly disordered material: orientational glass

To date most of our knowledge on tunneling dynamics of particles in solids comes from the extensive studies of crystalline or nearly crystalline materials. However, in reality, the crystalline state is the exception rather then the rule. Disorder exists in varying degree, ranging from a few impurities in an otherwise perfect crystalline host to the strongly disordered limit of allows or glassy structures. All the studies on muon and muonium localization so far have been focused on crystals with weak disorder [1]. In this section we present experimental studies of muonium tunneling dynamics under conditions of strong disorder in orientational glass [22,23].

The term «orientational glasses» usually refers to randomly diluted (or randomly mixed) molecular crystals. Molecular crystals without such randomness in their chemical constitution undergo an order-disorder phase transition from the «plastic crystal» phase at high temperatures, where the multipole moments associated with the molecules can rotate more or less freely, into a phase with a long-range orientational order at lower temperature (e.g. N_2, ortho-H_2, CH_4, CD_4, etc.). This order gets severely disturbed by dilution of the material with atomic species which have no multipole moment (e.g. Ar in N_2, Kr in CH_4, para-H_2 in ortho-H_2, etc.); strong enough dilution leads to a new type of phase, where the multipole moments are frozen into random directions. These glass phases are believed to result from the combined effect of the frustration of the highly anisotropic interactions between the molecules (e.g., electrostatic multipole-multipole) and the disorder introduced by the random substitution of molecular multipoles by non-interacting shperical atoms or molecules [22]. The frustration in these systems arises from the geometrical impossibility of realizing the minimum possible energy configuration for all pairs of neighboring molecular quadrupoles in close 3D lattices, and disorder simply comes from the replacement of multipole bearing molecules by non-interacting diluents such as Kr in the CH_4–Kr system.

Although orientational glasses have many common features with structural glasses (like amorphous SiO_2) and spin glasses (like CuMn) there is un important difference even in qualitative description of these glass systems. Unlike the canonical spin glasses such as

CuMn alloys for which the frustration and the disorder go hand-in-hand, the orientational glasses belong to a new class of systems characterized by independent effects of both frustration and disorder. The interaction between two molecules responsible for the orientational ordering (the short range highly anisotropic electric quadrupole-quadrupole or octopole-octopole interaction) is explicitly, known. This fact allows one to extract the influence of disorder which can be easily varied (or even switched on and off) by changing the temperature and/or composition, allowing a detailed investigation of the effects of strong disorder on quantum tunneling of muonium atoms.

Since the early heat-capacity measurements [24], it has been known that the specific-heat anomalies in CH_4 at the orientational transition vanish if a sufficient amount of Kr is added to CH_4. It has been established by heat-capacity, NMR [25] and dielectric techniques [26] that as the Kr concentration increases the temperature of orientational transition gradually decreases. Above the critical concentration (about 25%) ordered phase never forms. Instead, as the temperature goes down the dynamical orientational disorder eventually freezes into a static pattern of randomly oriented octupoles, the orientational glass.

Figure 2 shows the temperature dependencies of the muonium hop rate in pure CH_4 and CH_4 + 25% Kr, extracted in the regime of dynamical averaging using the values of δ obtained from the low temperature values of T_2^{-1} [10]. The plateaus in $\tau_c^{-1}(T)$ (around 45–55 K in pure CH_4 and 50–60 K in the mixture) manifest the onset of muonium band motion [1,5]. The bandwidth $\tilde{\Delta} \sim 10^{-2}$ K determined in CH_4 + 25% Kr mixture turns out to be remarkably high: it is only slightly less than $\tilde{\Delta} \sim 3 \cdot 10^{-2}$ K in pure CH_4, about the same as that in pure solid nitrogen [11] and an order of magnitude higher than $\tilde{\Delta} \sim 10^{-3}$ K in pure solid CD_4 [10]. Addition of 16% of Kr to CH_4 does not change the bandwidth for Mu tunneling dynamics. This fact suggests that substitution of 2 nearest neighbours out of 12 does not destroy the coherence in Mu band regime. This is a remarkable feature never observed in quantum diffusion studies so far: presence of impurities in a crystal even on the level of 10^{-3} is typically enough to destroy the coherent tunneling regime [1,5]. Although addition of 25% of Kr to CH_4 does change the muonium bandwidth, in the temperature range between 50 and 60 K Mu atom still exhibits coherent tunneling which means that substitution of 3 nearest neighbours out of 12 still does not destroy the coherence. The question why does such a high concentration of foreign atoms fail to destroy coherence in muonium dynamics still remains open.

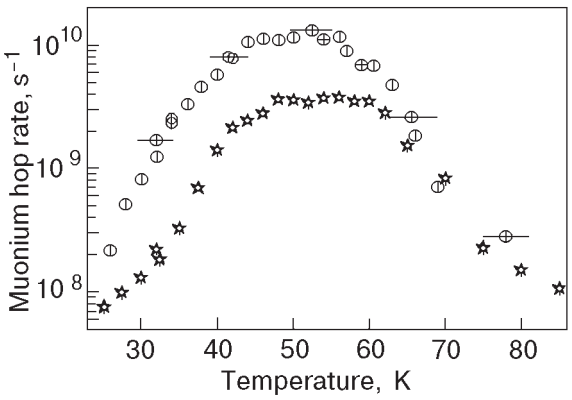

Fig. 2. Temperature dependencies of muonium hop rate in pure solid methane (circles) and solid mixture of CH_4 + + 25% Kr (stars).

3. Electron transport via μ^+SR

Ionization of matter by high energy charged particle radiation inevitably produces excess electrons and thus may cause electrical breakdown even in wide-gap insulating materials subjected to high electric field. These materials are used in a large number of applications ranging from power generation equipment to microelectronic devices. It is therefore important to understand the transport mechanisms of radiolysis electrons in insulators.

In condensed matter, the transport of a charged particle depends upon the adiabaticity of its interaction with excitations of the environment. For particles slow enough that electronic excitations are prohibited, the general picture depends critically on the interplay of two characteristic times. The first represents the typical time that a charged particle spends interacting with a given atom or molecule: $\tau_i = a/v$, where a is the lattice constant and v is the velocity of the charged particle. The other characteristic time is ω^{-1}, where $\hbar\omega$ is the characteristic phonon energy. Fast particles ($\omega\tau_i << 1$) move through the medium retaining their «bare» identity, whereas charge carriers moving so slowly that $\omega\tau_i > 1$ are followed «instantaneously» by phonon modes and are best thought of as a polaron [27] whose mobility is drastically decreased. This crossover from the fast ($\omega\tau_i < 1$) to the slow ($\omega\tau_i > 1$) regime thus leads to a dramatic change in charge transport properties.

In different insulators, electron transport is determined by qualitatively different interactions of electrons with the medium. Measurements on Ar, Kr and Xe crystals [28,29] show clearly that electron mobilities in these solids are comparable to those found in wide-band semiconductors ($b_e \sim 10^3$ cm^2 s^{-1}V^{-1}), which encouraged different authors to apply Shockley's well-known theory [30]. An approxima-

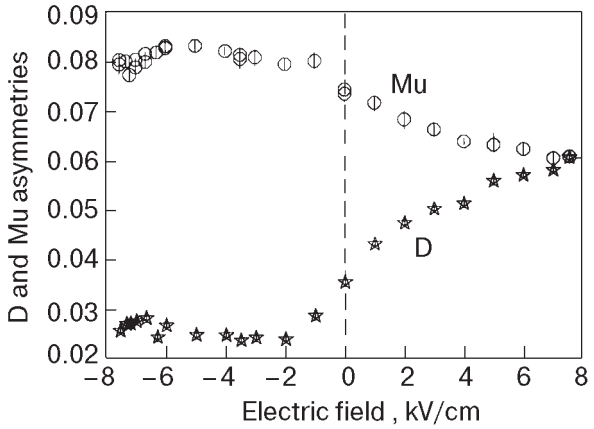

Fig. 3. Electric field dependences of muonium (Mu, circles) and diamagnetic (D, stars) amplitudes in α-N_2 at T = 20 K.

tion in which the free charge carriers are completely delocalized and the electron-phonon interaction is treated as a perturbation gave an adequate description of the observed electron transport.

The rather low electron mobilities found in the diatomic solids of N_2, CO, and O_2 [31] ($b_e \sim 10^{-2} - 10^{-3}$ $cm^2s^{-1}V^{-1}$) suggest that a fundamentally different mechanism of electron transport occurs in these materials. The localization of excess electrons with the formation of a small polaron [27] due to strong interactions with excitations of the medium was proposed to explain such low values of drift mobility.

Measurements of electron mobility by time-of-flight (TOF) technique represent a very direct approach to the study of charge transport properties in solids. It should be noted, however, that in such experiments the path length between electrodes is macroscopic ($\sim 10^{-2}$–10^{-1} cm), making the results highly susceptible to spurious TOF changes if electrons interact with crystalline defects such as impurities, strains, and microcracks. The muon spin rotation technique avoids these difficulties inherent to the traditional TOF technique because the distances involved are much shorter ($\sim 10^{-6} - 10^{-4}$ cm).

In μSR experiments each incoming several-MeV μ^+ leaves behind an ionization track of liberated electrons and ions. Although this circumstance has been disregarded in a great majority of experimental and theoretical studies of condensed matter by μ^+SR techniques, the liberation of electrons by muon radiolysis is far from a negligible effect — in fact, in some insulators and semiconductors it may determine much of the subsequent behaviour of the system. Recent μ^+SR, experiments in liquid helium [32], solid nitrogen [33–36], liquid [37] and solid neon and argon [29,38] have shown that the spatial distribution of the ionization track products is highly anisotropic with respect to the final position of the muon: the μ^+ thermalizes well «downstream» from the end of its track. Some of the excess electrons generated in this track turn out to be mobile enough to reach the thermalized muon and form the hydrogen-like muonium ($Mu \equiv \mu^+e^-$) atom.

The phenomenon of delayed muonium formation (DMF) described above is crucially dependent on electron interaction with the environment through its influence on electron mobility. Thus DMF forms the basis of a new technique [34] for measurements of the electron mobility b_e in insulators [36–38] and semiconductors [39–41] on a microscopic scale: b_e can be estimated whenever one can measure both the characteristic time for Mu atom formation and the characteristic distance between the stopped muon and its «last» radiolysis electron. In this section we consider several examples where μ^+SR techniques allow one to determine whether excess electron in cryocrystals becomes a polaron or occupies the conduction band (in other words, whether electron is localized or delocalized).

3.1. Electron delocalization in solid α-nitrogen

Both muonium (Mu) and diamagnetic (D) signals are evident in solid N_2 at all temperatures [33]. We found strong correlation between the muonium amplitude and the electron mobility in solid nitrogen: both have similar temperature dependences. The straightforward implication is that Mu formation in *s*-N_2 is at least partially due to convergence of the μ^+ and a radiolysis electron. In *s*-N_2 positive charges have been found to be immobile [31], so the e^- must move to the μ^+.

Rather strong evidence in support of this picture comes from the electric field dependences of the diamagnetic and Mu amplitudes (Fig. 3). A positive sign for E signifies that the electric field is applied in the same direction as the initial muon momentum. The results show that, on average, muons thermalize downstream from the last radiolysis electrons of the muon's ionization track; in this case a positive E will pull the μ^+ and e^- apart, giving rise to an increased D amplitude, whereas a negative E will push the μ^+ and e^- together. The characteristic muon-electron distance R in solid α-N_2 was estimated from these measurements to be about $5 \cdot 10^{-6}$ [34,35]. Analogous measurements in β-N_2 at T = 59 K reveled a much weaker electric field dependence, giving an estimate of the characteristic μ^+—e^- distance of about half that in α-N_2 [36]. The characteristic time τ for e^- transport to the μ^+ can be determined by measurement of the magnetic field dependence of the Mu amplitude. Assuming that the muonium formation process is governed by a first-order kinetic equation $dn_{Mu}(t) = -dn_{\mu}(t) = \lambda n_{\mu}(t)$, where $\lambda \equiv 1/\tau$ is the characteristic formation rate, the muonium amplitude has been shown to be

$$A_{\mathrm{Mu}} \propto \frac{\lambda}{\sqrt{\lambda^2 + \omega_{\mathrm{Mu}}^2}}. \qquad (7)$$

For a weak local electric field E the electron mobility b_e is independent of E and the charge drift velocity v is defined by

$$v = b_e E. \qquad (8)$$

In the absence of an applied field, the electric field at a distance r from the muon is $E = e/\epsilon r^2$, which can be integrated to give an expression for the Mu formation time

$$\tau = \frac{R^3 \epsilon}{3eb_e}. \qquad (9)$$

Very near the muon, E is large and b_e is no longer constant; however, Eq. (9) turns out to be a good approximation anyway because τ is determined mainly by slow motion at large distances in low electric fields. Expressions (7) and (9) allow one to estimate the electron mobility b_e.

Figure 4 shows the magnetic field dependence of A_{Mu} in α-N_2 (circles) and in β-N_2 (stars). In β-N_2 the estimate of the electron mobility from μ^+SR measurements using Eqs. (7) and (9) gives a value of the same order of magnitude as that extracted by time-of-flight technique. The dashed curve shows numerical calculations according to Eqs. (7) and (9) with the values of electron mobility determined from TOF measurements [31] in α-N_2. The experiment, however, show that A_{Mu} is field independent (i.e. $\lambda >> \omega_{\mathrm{Mu}}$), which means that the Mu formation time is much shorter than expected from TOF measurements. Using Eq. (7) one can estimate a lower limit for the electron mobility in α-N_2: $b_e > 100$ cm^{2}s^{-1}V^{-1} — a value more than 10^5 times higher than the electron mobility in

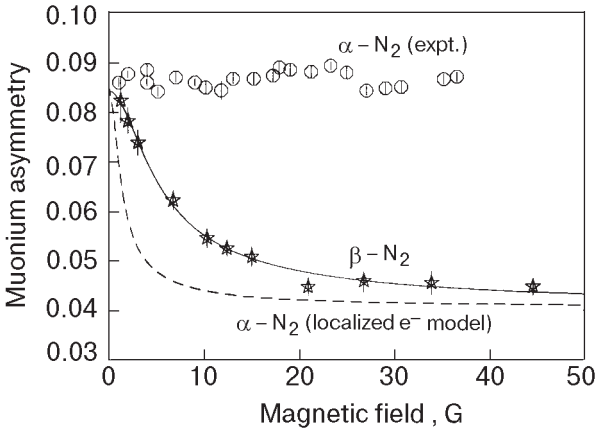

Fig. 4. Magnetic field dependences of muonium amplitudes in α-N_2 at T = 20 K (circles) and in β-N_2 at T = 59 K (stars). Smooth curves represent numerical calculations in the framework of a localized electron model (see text).

β-N_2. The discrepancy between TOF and μ^+SR results in α-N_2 is probably connected to crystal cracking at the α—β transition of *s*-N_2. The TOF technique [31], which relies on electron drift over the macroscopic distances between electrodes, is inevitably sensitive to crystal imperfections. We claim that the μ^+SR technique, which involves microscopic characteristic distances, avoids these difficulties. Such a high electron mobility suggests that the electron transport mechanism in α-N_2 is fundamentally different from that in β-N_2. Probably the localization of electrons does not occur in α-N_2 and Shockley's delocalized approximation [30] can be applied. A possible mechanism for electron localization in β-N_2 may be interactions with the rotational modes of N_2 molecules — a scattering mechanism that is absent in α-N_2 due to the orientational ordering of the molecules.

3.2. Electron localization in orientational glass

Most of our understanding of electron transport in solids is modelled on nearly perfect crystalline materials, but even in this limit disorder plays a crucial role [42]. The most familiar phenomenon governing electron transport in disordered metals is «Anderson localization» [4]: introduction of sufficiently strong disorder into a metallic system causes spatial localization of electron states near the Fermi level and thus drives a transition to an insulating state. In metals, however, electron-electron interactions dramatically modify the density of states at the Fermi level, leading to formation of the Coulomb pseudogap [43]. To observe the effects of disorder on electron transport without the complications of electron-electron interactions, one must therefore study electron dynamics in a disordered insulating host [44].

Orientational glasses formed by random mixtures of molecular and atomic species [22] offers a unique opportunity for such studies. One of the best studied orientational glass systems is the N_2–Ar mixture [45]. Pure N_2 has two low-pressure crystalline forms, the hexagonal close-packed (hcp) high temperature phase and the cubic *Pa*3 (fcc) low temperature phase. Despite intrinsic geometrical frustration, pure N_2 undergoes a first-order phase transition to a long-range periodic orientationally ordered α-phase below $T_{\alpha\beta}$ = 35.6 K; the high temperature β-phase is orientationally disordered.

Solid $(N_2)_{1-x}Ar_x$ is obtained by simply cooling liquid mixtures, as nitrogen and argon are completely miscible. As the Ar concentration x is increased, the hcp-to-fcc transition temperature decreases. Above the critical Ar concentration $x_c \approx 0.23$, the hcp lattice appears to be stable down to T = 0. The dynamical orientational disorder of the high-T phase eventually

freezes into a static pattern of randomly oriented N_2 molecules, the orientational glass [45].

Being a mixture of insulators, the N_2–Ar system has a very large energy gap ($\sim$ 10 eV), so that even at high temperature the ambient density of free electronic states is exponentially low. Experimental study of electron transport in this system therefore requires that the empty conduction band be «injected» with free carriers, ideally in low enough concentrations that electron-electron interactions can be safely ignored. The ionization of molecules and/or atoms by high energy charged particles (e.g. positive muons) offers just such a source of free carriers.

Figure 5 depicts the temperature dependences of the asymmetries (amplitudes) of the various signals in solid $(N_2)_{1-x}Ar_x$ for x = 0, 0.09, 0.16, and 0.25. At high temperature (above about 40 K), all the mixtures have roughly the same Mu and μ_D asymmetries as pure N_2. At low temperatures, however, adding argon causes dramatic changes. In pure N_2 below about 30 K there is a large Mu signal and a small μ_D signal, indicating efficient DMF; as Ar is added there is a progressively larger μ_D signal, indicating reduced DMF, until at x = 0.25 there is only a small Mu signal. In solid N_2 muonium formation has been shown [34, 36]

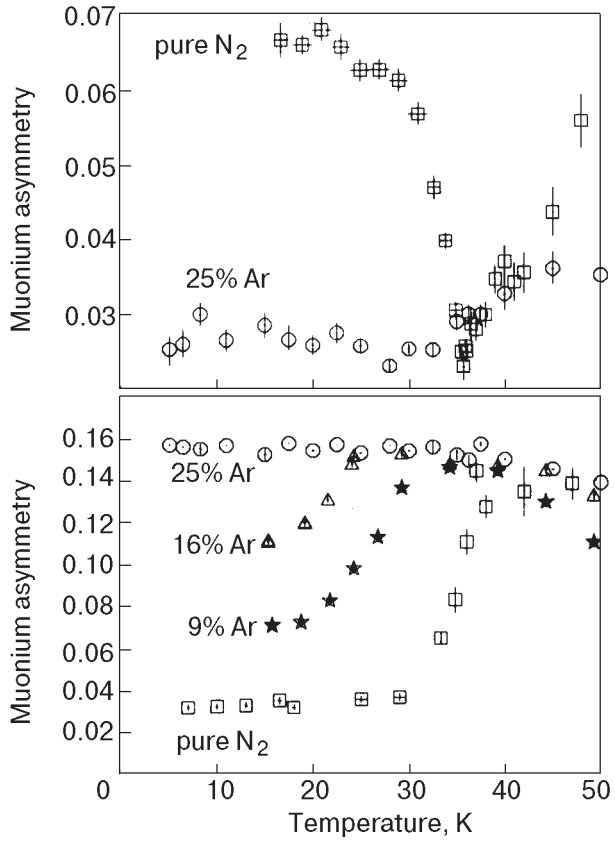

Fig. 5. Temperature dependences of muonium (top, $H \approx 5$ G) and diamagnetic (bottom, $H \approx 100$ G) signal amplitudes in pure solid nitrogen (squares) and solid $(N_2)_{1-x}Ar_x$ (circles: x = 0.25; triangles: x = 0.16; stars: x = 0.09).

to proceed via two channels: the thermal DMF process outlined above and the epithermal prompt process which takes place prior to the μ^+ thermalization and is therefore independent of temperature, electron mobility, etc. The small, temperature independent Mu amplitude in the x = 0.25 sample (see Fig. 5) is the same as the prompt Mu amplitude in pure solid nitrogen [36], suggesting a complete absence of DMF in the orientational glass.

The hypothesis that Mu formation in the x = 0.25 mixture is essentially all via the prompt channel at 20 K is further supported by the observation that A_{Mu} and A_D do not depend on an externally applied electric field for that, sample, as shown in Fig. 6. Both amplitudes show significant electric field dependence in pure N_2 at 20 K, from which the characteristic muon-electron distance R is estimated to be about 50 nm [34,36]; about the same value of R is found in solid Ar, which exhibits almost 100% DMF [38]. The absence of DMF at this length scale at low temperature in the x = 0.25 mixture suggests that electrons are localized in orientational glass [44].

4. Conclusions

Recent studies on both quantum diffusion of muonium atom and electron transport in condensed matter have demonstrated considerable power of muon spin relaxation techniques in determination of the quantum state of these particles. The dynamics of neutral and charged particles is basically governed by different mechanisms of localization and delocalization.

This work was supported by the INTAS Foundation, the Royal Society of London, NSF, and NATO.

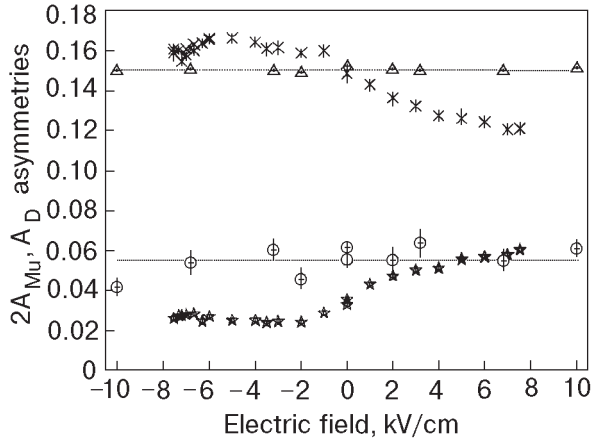

Fig. 6. Electric field dependences of $2A_{Mu}$ and A_D in pure solid nitrogen (crosses and stars, respectively) and in solid 75% N_2 + 25% Ar (circles and triangles, respectively) in a transverse magnetic field H = 36 G at T = 20 K. The muoniuin amplitudes are doubled to compensate for the 50% depolarization of Mu by hyperfine oscillations [2].

1. V.G. Storchak and N.V. Prokof'ev, *Rev. Mod. Phys.* **70**, 929 (1998).
2. A. Schenck, *Muon Spin Rotation: Principles and Applications in Solid State Physics*, Adam Hilger, Bristol (1986); S.F.J. Cox, *J. Phys.* **C20**, 3187 (1987); J.H. Brewer, *Muon Spin Rotation/Relaxation/Resonance*, in: *Encyclopedia of Applied Physics*, G.L. Trigg (ed.), VCH, New York (1995).
3. A.O. Caldeira and A.J. Leggett, *Phys. Rev. Lett.* **46**, 211 (1981); *Ann. Phys. (N.Y.)* **149**, 374 (1983).
4. P.W. Anderson, *Phys. Rev.* **109**, 1492 (1958).
5. Yu.M. Kagan and N.V. Prokof'ev, *Quantum Tunneling Diffusion in Solids*, in: *Quantum Tunneling in Condensed Media*, A.J. Leggett and Yu.M. Kagan (eds.) North-Holland (1992), p.37.
6. A.F. Andreev and I.M. Lifshitz, *Zh. Eksp. Teor. Fiz.* **56**, 2057 (1969) [*Sov. Phys. JETP* **29**, 1107 (1969)].
7. R.A. Guyer and L.I. Zane, *Phys. Rev.* **188**, 445 (1969).
8. L.D. Landau and E.M. Lifshitz, *Quantum Mechanics. Non Relativistic Theory*, Nauka, Moscow (1974).
9. A.J. Leggett et. al., *Rev. Mod. Phys.* **59**, 1 (1987).
10. V.G. Storchak et. al., *Phys. Rev. Lett.* **82**, 2729 (1999).
11. V.G. Storchak, J.H. Brewer, W.N. Hardy, S.R. Kreitman, and G.D. Morris, *Phys. Rev. Lett.* **72**, 3056 (1994).
12. R. Kadono in: *Perspectives in Meson Science*, T. Yamazaki, K. Nakai, and K. Nagamine (eds.) North-Holland, Amsterdam (1992), p. 113.
13. S.F.J. Cox and D.S. Sivia, *Hyperfine Int.* **87**, 971 (1994).
14. C.P. Slichter, *Principles of Magnetic Resonance*, Springer-Verlag, Berlin (1980).
15. D. Steinbinder et.al., *Europhys. Lett.* **6**, 535 (1988).
16. J. Kondo, *Physica* **B125**, 279 (1984); **B126**, 377 (1984); K. Yamada, *Prog. Theor. Phys.* **72**, 195 (1984).
17. R. Kadono, *Hyperfine Int.* **64**, 615 (1990).
18. P.C.E. Stamp and C. Zhang, *Phys. Rev. Lett.* **66**, 1902 (1991).
19. Yu.M. Kagan and N.V. Prokof'ev, *Phys. Lett.* **A150**, 320 (1990).
20. D.G. Eshchenko, V.G. Storchak, J.H. Brewer, S.P. Cottrell, S. F.Y. Cox, E. Karlsson, and Waeppling, *Fiz. Nizk. Temp.* **27**, 1153 (2001) [Low Temp. Phys. 27, 854 (2001)].
21. M.G. Richards et. al., *J. Low Temp. Phys.* **24**, 1 (1976); V.A. Mikheev, B.N. Esel'son, V.N. Grigor'ev and N.P. *Mikihn, Fiz. Nizk. Temp.* **3**, 387 (1977) [*Sov. J. Low. Temp. Phys.* **3** (1977)].
22. U.T. Hochli, K. Knorr, and A. Loidl, *Adv. Phys.* **39**, 405 (1990).
23. K. Binder and J.D. Reger, *Adv. Phys.* **41**, 547 (1992).
24. A. Eucken and H. Veith, *Z. Phys. Chem.* **B34**, 275 (1936).
25. P. Calvani et. al., *Phys. Lett.* **A86**, 490 (1981).
26. R. Bohmer and A. Loidl, *Z. Phys.* **B80**, 139 (1990).
27. T. Holstein, *Ann. Phys.* **8**, 343 (1959).
28. L.S. Miller, S. Howe, and W.E. Spear, *Phys. Rev.* **166**, 871 (1968).
29. D.G. Eshchenko, V.G. Storchak, J.H. Brewer et. al., *Phys. Rev.* **B66**, 035105 (2002).
30. W. Shockley, *Bell System Tech. J.* **30**, 900 (1951).
31. R.J. Loveland, P.L. Le Comber, and W.E. Spear, *Phys. Rev.* **B6**, 3121 (1972).
32. E. Krasnoperov, E. Meilikhov, R. Abela, D. Herlach, E. Morenzoni, F. Gydax, A. Schenck, and D.G. Eshchenko, *Phys. Rev. Lett.* **69**, 1560 (1992).
33. V. Storchak, J.H. Brewer, and G.D. Morris, *Phys. Lett.* **A193**, 199 (1994).
34. V. Storchak, J.H. Brewer, and G.D. Morris, *Phys. Rev. Lett.* **75**, 2384 (1995).
35. V. Storchak, J.H. Brewer, and G.D. Morris, *Phil. Mag.* **72**, 241 (1995).
36. V. Storchak, J.H. Brewer, G.D. Morris, D.J. Arseneau, and M. Senba, *Phys. Rev.* **B59**, 10559 (1999).
37. V. Storchak, J.H. Brewer, and G.D. Morris, *Phys. Rev. Lett.* **76**, 2969 (1996).
38. V. Storchak, J.H. Brewer, and D.G. Eshchenko, *Appl. Mag. Reson.* **13**, 15 (1997).
39. V.G. Storchak et. al., *Phys. Rev. Lett.* **78,** 2835 (1997).
40. D.G. Eshchenko, V.G. Storchak, and G.D. Morris, *Phys. Lett.* **A264**, 226 (1999).
41. D.G. Eshchenko, V.G. Storchak, J.H. Brewer, and R.L. Lichti, *Phys. Rev. Lett.*, in press.
42. N.F. Mott and E.A. Davis, *Electron Processes in Non-Crystalline Materials*, Clarendon Press, Oxford (1979).
43. N.F. Mott, *Metal-Insulator Transitions*, Taylor and Francis, London (1974).
44. V.G. Storchak, D.G. Eshchenko, J.H. Brewer, G.D. Morris, S.P. Cottrell, and S.F.J. Cox, *Phys. Rev. Lett.* **85**, 166 (2000).
45. J.A. Hamida, E.B. Genio, and N.S. Sullivan, *J. Low Temp. Phys.* **103**, 49 (1996).